American Mineralogist, Volume 99, pages 1155–1162, 2014

Vanadio-oxy-chromium-dravite, $NaV_3(Cr_4Mg_2)(Si_6O_{18})(BO_3)_3(OH)_3O$, a new mineral species of the tourmaline supergroup

Ferdinando Bosi[1,3,*], Leonid Reznitskii[2], Henrik Skogby[3] and Ulf Hålenius[3]

[1]Dipartimento di Scienze della Terra, Sapienza Università di Roma, P.le A. Moro, 5, I-00185 Rome, Italy
[2]Russian Academy of Science, Siberian Branch, Institute of the Earth's Crust, Lermontova strasse, 128, Irkutsk, Russia
[3]Department of Geosciences, Swedish Museum of Natural History, Box 50007, SE-10405 Stockholm, Sweden

Abstract

Vanadio-oxy-chromium-dravite, $NaV_3(Cr_4Mg_2)(Si_6O_{18})(BO_3)_3(OH)_3O$, is a new mineral of the tourmaline supergroup. It is found in metaquartzites of the Pereval marble quarry (Sludyanka, Lake Baikal, Russia) in association with quartz, Cr-V-bearing tremolite and muscovite-celadonite-chromphyllite-roscoelite, diopside-kosmochlor-natalyite, Cr-bearing goldmanite, escolaite-karelianite, dravite-oxy-vanadium-dravite, V-bearing titanite and rutile, ilmenite, oxyvanite-berdesinskiite, shreyerite, plagioclase, scapolite, zircon, pyrite, and an unnamed oxide of V, Cr, Ti, U, and Nb. Crystals are emerald green, transparent with a vitreous luster, pale green streak, and conchoidal fracture. Vanadio-oxy-chromium-dravite has a Mohs hardness of approximately 7½, and a calculated density of 3.3 g/cm^3. In plane-polarized light, vanadio-oxy-chromium-dravite is pleochroic (O = dark green, E = pale green) and uniaxial negative: $\omega = 1.767(5)$, $\varepsilon = 1.710(5)$. Vanadio-oxy-chromium-dravite is rhombohedral, space group $R3m$, with the unit-cell parameters $a = 16.1260(2)$, $c = 7.3759(1)$ Å, $V = 1661.11(4)$ Å^3, $Z = 3$. Crystal chemistry analysis resulted in the empirical structural formula:

$^{X}(Na_{0.89}K_{0.06}\square_{0.05})\ ^{Y}(V^{3+}_{2.77}Mg_{0.17}Fe^{3+}_{0.06})\ ^{Z}(Cr^{3+}_{1.85}Al_{1.59}V^{3+}_{0.78}Mg_{1.78})\ ^{T}[(Si_{5.95}Al_{0.05})O_{18}]$
$^{B}(BO_3)_3\ ^{V}(OH_{2.91}O_{0.09})\ ^{W}(O_{0.86}F_{0.14})$.

The crystal structure of vanadio-oxy-chromium-dravite was refined to a statistical index $R1$ of 1.16% using 2543 unique reflections collected with Mo$K\alpha$ X-radiation. Ideally, vanadio-oxy-chromium-dravite is related to oxy-chromium-dravite and oxy-vanadium-dravite by the homovalent substitution $V^{3+} \leftrightarrow Cr^{3+}$. Tourmaline with chemical compositions classified as vanadio-oxy-chromium-dravite can be either Cr^{3+}-dominant or V^{3+}-dominant as a result of the compositional boundaries along the solid solution between Cr^{3+} and V^{3+} that are determined at $^{Y+Z}(V_5Cr_2)$, corresponding to $Na^{Y}(V_3)^{Z}(V_2Cr_2Mg_2)Si_6O_{18}(BO_3)_3(OH)_3O$, and $^{Y+Z}(V_{1.5}Cr_{5.5})$, corresponding to $Na^{Y}(V_{1.5}Cr_{1.5})^{Z}(Cr_4Mg_2)Si_6O_{18}(BO_3)_3(OH)_3O$.

Keywords: Vanadio-oxy-chromium-dravite, tourmaline, new mineral species, crystal-structure refinement, electron microprobe, infrared spectroscopy, optical absorption spectroscopy

Introduction

The tourmaline supergroup minerals are widespread, occurring in sedimentary, igneous, and metamorphic settings. They are important indicator minerals that can provide information on the compositional evolution of their host rocks, chiefly due to their ability to incorporate a large number of elements (e.g., Novák et al. 2004, 2011; Agrosì et al. 2006; Lussier et al. 2011a; van Hinsberg et al. 2011; Bačík et al. 2012). However, the chemical composition of tourmalines is also controlled by short-range and long-range constraints (e.g., Hawthorne 1996, 2002; Bosi and Lucchesi 2007; Bosi 2010, 2011, 2013; Henry and Dutrow 2011; Skogby et al. 2012) as well as by temperature (van Hinsberg and Schumacher 2011). Tourmaline supergroup minerals are complex borosilicates and their crystal structure and crystal chemistry have been extensively studied (e.g., Foit 1989; Hawthorne and Henry 1999; Bosi and Lucchesi 2007; Lussier et al. 2008, 2011b; Bosi 2008; Bosi et al. 2010; Filip et al. 2012). In accordance with Henry et al. (2011), the general formula of tourmaline may be written as: $XY_3Z_6T_6O_{18}(BO_3)_3V_3W$, where X ($\equiv {}^{[9]}X$) = Na^+, K^+, Ca^{2+}, $\square$ (= vacancy); Y ($\equiv {}^{[6]}Y$) = Al^{3+}, Fe^{3+}, Cr^{3+}, V^{3+}, Mg^{2+}, Fe^{2+}, Mn^{2+}, Li^+; Z ($\equiv {}^{[6]}Z$) = Al^{3+}, Fe^{3+}, Cr^{3+}, V^{3+}, Mg^{2+}, Fe^{2+}; T ($\equiv {}^{[4]}T$) = Si^{4+}, Al^{3+}, B^{3+}; B ($\equiv {}^{[3]}B$) = B^{3+}; W ($\equiv {}^{[3]}O1$) = OH^{1-}, F^{1-}, O^{2-}; V ($\equiv {}^{[3]}O3$) = OH^{1-}, O^{2-} and where, for example, T represents a group of cations (Si^{4+}, Al^{3+}, B^{3+}) accommodated at the [4]-coordinated T sites. The dominance of these ions at one or more sites of the structure gives rise to a range of distinct mineral species.

Recently, several new minerals of the tourmaline supergroup were approved by the Commission on New Minerals, Nomenclature and Classification (CNMNC) of the International Mineralogical Association (IMA). Among these are several oxy-tourmalines related by the complete solid solution in the Al^{3+}-Cr^{3+}-V^{3+} subsystem: oxy-dravite, end-member formula $NaAl_3(Al_4Mg_2)(Si_6O_{18})(BO_3)_3(OH)_3O$ (IMA 2012-004a; Bosi and Skogby 2013), oxy-

* E-mail: ferdinando.bosi@uniroma1.it

chromium-dravite, $NaCr_3(Cr_4Mg_2)(Si_6O_{18})(BO_3)_3(OH)_3O$ (IMA 2011-097; Bosi et al. 2012a); oxy-vanadium-dravite, $NaV_3(V_4Mg_2)(Si_6O_{18})(BO_3)_3(OH)_3O$ (IMA 11-E; Bosi et al. 2013a).

A new species of oxy-tourmaline, vanadio-oxy-chromium-dravite, has been approved by the Commission on New Minerals, Nomenclature and Classification of the International Mineralogical Association (IMA 2012-034). The holotype specimen (sample PR76) is deposited in the collections of the Museum of Mineralogy, Earth Sciences Department, Sapienza University of Rome, Italy, catalog number 33067. A formal description of the new species vanadio-oxy-chromium-dravite (V^{3+}-rich tourmaline) is presented here, including a full characterization of its physical, chemical, and structural properties. After the sample PR76 (Cr_2O_3 = 12.9 wt%) was approved as a new mineral species by the CNMNC-IMA, another sample (PR1973) showing higher contents of Cr_2O_3 (24.5 wt%) was found from the same locality. The composition of latter sample is closer to the vanadio-oxy-chromium-dravite end-member. Consequently, we will here present chemical and structural data for both of these samples.

Occurrence, appearance, and physical and optical properties

The crystals of vanadio-oxy-chromium-dravite occur in metaquartzites in the Pereval marble quarry, Sludyanka crystalline complex, Southern Baikal region, Russia (51°37′N 103°38′E). The Pereval quarry is the type locality (see Bosi et al. 2012a for a more detailed description) for natalyite, florensovite, kalininite, magnesiocoulsonite, oxy-vanadium-dravite, batisivite, oxyvanite, and cuprokalininite. Minerals associated with the holotype specimen PR76 are: quartz, Cr-V-bearing tremolite, and dioctahedral mica (muscovite-celadonite-chromphyllite-roscoelite), diopside-kosmochlor-natalyite, Cr-bearing goldmanite, escolaite-karelianite, dravite-oxy-vanadium-dravite, V-bearing titanite and rutile, ilmenite, oxyvanite-berdesinskiite, shreyerite, plagioclase, scapolite, zircon, pyrite, and an unnamed oxide of V, Cr, Ti, U, and Nb, whereas minerals associated with sample PR1973 are: quartz, calcite, Cr-V-bearing diopside, and tremolite, V-bearing magnesiochromite, goldmanite-uvarovite, karelianite-escolaite, and V-Cr tourmalines. The host rocks (quartz-diopside) are Cr-V-bearing carbonate-siliceous sediments, metamorphosed to granulite facies and partly diaphtorized to amphibolite facies (retrograde stage). Vanadio-oxy-chromium-dravite was formed in the prograde stage (granulite facies). The crystals are euhedral, reaching up to 0.3 mm in length, and may be chemically zoned, but homogeneous crystals also occur.

The vanadio-oxy-chromium-dravite morphology consists of elongated $\{10\bar{1}0\}$ and $\{11\bar{2}0\}$ prisms terminated by a prominent {0001} pedion and small, minor $\{10\bar{1}1\}$ pyramidal faces. Crystals are emerald green, with pale green streak, transparent and display vitreous luster. They are brittle and show conchoidal fracture. The Mohs hardness is approximately 7½ (Reznitsky et al. 2001). The calculated density is 3.279 and 3.313 g/cm^3 for samples PR76 and PR1973, respectively. In transmitted light, vandio-oxy-chromium-dravite is pleochroic with O = dark green and E = pale green. Vanadio-oxy-chromium-dravite is uniaxial negative with refractive indices, measured by the immersion method using white light from a tungsten source, of $\omega = 1.767(5)$, $\varepsilon = 1.710(5)$ (sample PR76).

Method

Single-crystal structural refinement

As mentioned previously, two crystals of the mineral (from holotype sample PR76 and specimen PR1973, which is closer to end-member composition) were selected for X-ray diffraction measurements on a Bruker KAPPA APEX-II single-crystal diffractometer, at Sapienza University of Rome (Earth Sciences Department), equipped with a CCD area detector (6.2 × 6.2 cm^2 active detection area, 512 × 512 pixels) and a graphite crystal monochromator, using Mo$K\alpha$ radiation from a fine-focus sealed X-ray tube. The sample-to-detector distance was 4 cm. A total of ca. 2500–3500 exposures (step = 0.2°, time/step = 20 s) covering a full reciprocal sphere with a redundancy of about 8 was used. Final unit-cell parameters were refined by means of the Bruker AXS SAINT program using reflections with $I > 10\ \sigma(I)$ in the range $5° < 2\theta < 78°$. The intensity data were processed and corrected for Lorentz, polarization, and background effects with the APEX2 software program of Bruker AXS. The data were corrected for absorption using the multi-scan method (SADABS). The absorption correction led to a significant improvement in R_{int}. No violations of $R3m$ symmetry were noted.

Structural refinement was done with the SHELXL-97 program (Sheldrick 2008). Starting coordinates were taken from Bosi et al. (2004). Variable parameters were: scale factor, extinction coefficient, atomic coordinates, site scattering values, and atomic displacement factors. To obtain the best values of statistical indexes ($R1$, $wR2$), a fully ionized scattering curve for O was used, whereas neutral scattering curves were used for the other atoms. In detail, the X and Y site were modeled by using Na and V scattering factors (respectively), while the occupancy of the Z site was modeled considering the presence of Cr and Mg. The T and B sites were modeled, respectively, with Si and B scattering factors and with a fixed occupancy of 1, because refinement with unconstrained occupancies showed no significant deviations from this value. Three full-matrix refinement cycles with isotropic displacement parameters for all atoms were followed by anisotropic cycles until convergence was attained. No significant correlations over a value of 0.7 between the parameters were observed at the end of refinement. Table 1 lists crystal data, data collection information, and refinement details; Table 2 gives the fractional atomic coordinates and site occupancies; Table 3 gives the displacement parameters; Table 4 gives selected bond distances. (A CIF[1] is available.)

[1] Deposit item AM-14-504, CIF. Deposit items are stored on the MSA web site and available via the *American Mineralogist* Table of Contents. Find the article in the table of contents at GSW (ammin.geoscienceworld.org) or MSA (www.minsocam.org), and then click on the deposit link.

Table 1. Single-crystal X-ray diffraction data details for vanadio-oxy-chromium-dravite

Sample	PR76	PR1973
Crystal size (mm)	0.10 × 0.12 × 0.18	0.14 × 0.15 × 0.18
a (Å)	16.1260(2)	16.1307(5)
c (Å)	7.3759(1)	7.3792(2)
V (Å^3)	1661.11(4)	1662.82(9)
Range for data collection, 2θ (°)	5–78	5–73
Reciprocal space range hkl	$-24 \le h \le 24$	$-26 \le h \le 26$
	$-28 \le k \le 27$	$-26 \le k \le 26$
	$-12 \le l \le 12$	$-8 \le l \le 12$
Total number of frames	2543	3681
Set of measured reflections	8934	13850
Unique reflections, R_{int} (%)	2135, 1.50	1769, 1.55
Redundancy	8	14
Absorption correction method	SADABS	SADABS
Refinement method	Full-matrix least-squares on F^2	Full-matrix least-squares on F^2
Structural refinement program	SHELXL-97	SHELXL-97
Extinction coefficient	0.00002(7)	0.00043(7)
Flack parameter	0.05(1)	0.019(9)
$wR2$ (%)	3.08	2.85
$R1$ (%) all data	1.16	1.15
$R1$ (%) for $I > 2\sigma(I)$	1.13	1.14
GooF	1.094	1.057
Largest diff. peak and hole (±e$^-$/Å^3)	0.28 and –0.28	0.45 and –0.37

Notes: R_{int} = merging residual value; $R1$ = discrepancy index, calculated from F-data; $wR2$ = weighted discrepancy index, calculated from F^2-data; GooF = goodness of fit; Diff. peaks = maximum and minimum residual electron density. Radiation, Mo$K\alpha$ = 0.71073 Å. Data collection temperature = 293 K. Space group $R3m$; $Z = 3$.

TABLE 2. Fractional atom coordinates and site occupancy for vanadio-oxy-chromium-dravite

Sample	PR76				PR1973			
Site	*x*	*y*	*z*	Site occupancy	*x*	*y*	*z*	Site occupancy
X	0	0	0.22494(15)	$Na_{1.002(6)}$	0	0	0.22692(17)	$Na_{0.993(6)}$
Y	0.123130(14)	0.061565(7)	0.63864(4)	$V_{0.974(2)}$	0.123155(12)	0.061578(6)	0.63896(4)	$V_{1.00}$
Z	0.298154(12)	0.261863(13)	0.60991(4)	$Cr_{0.436(2)}Mg_{0.564(2)}$	0.297932(11)	0.261752(11)	0.60924(4)	$Cr_{0.510(2)}Mg_{0.490(2)}$
B	0.10977(5)	0.21953(9)	0.45462(16)	$B_{1.00}$	0.10942(4)	0.21884(9)	0.4548(2)	$B_{1.00}$
T	0.189705(15)	0.188037(15)	0	$Si_{1.00}$	0.189452(14)	0.187791(15)	0	$Si_{1.00}$
O1	0	0	0.76569(18)	$O_{1.00}$	0	0	0.7652(2)	$O_{1.00}$
O2	0.06061(3)	0.12122(6)	0.48951(12)	$O_{1.00}$	0.06032(3)	0.12064(6)	0.49075(14)	$O_{1.00}$
O3	0.25651(7)	0.12825(3)	0.50956(12)	$O_{1.00}$	0.25529(6)	0.12764(3)	0.50895(15)	$O_{1.00}$
O4	0.09232(3)	0.18464(7)	0.07058(12)	$O_{1.00}$	0.09231(3)	0.18461(7)	0.07087(15)	$O_{1.00}$
O5	0.18250(7)	0.09125(3)	0.08897(11)	$O_{1.00}$	0.18224(6)	0.09112(3)	0.08972(13)	$O_{1.00}$
O6	0.19178(4)	0.18257(4)	0.78153(8)	$O_{1.00}$	0.19107(4)	0.18184(4)	0.78175(10)	$O_{1.00}$
O7	0.28213(4)	0.28199(4)	0.07413(8)	$O_{1.00}$	0.28211(4)	0.28189(4)	0.07298(10)	$O_{1.00}$
O8	0.20690(4)	0.26768(5)	0.43845(9)	$O_{1.00}$	0.20637(4)	0.26689(4)	0.43761(11)	$O_{1.00}$
H3	0.2676(14)	0.1338(7)	0.396(2)	$H_{1.00}$	0.2606(14)	0.1303(7)	0.393(3)	$H_{1.00}$

TABLE 3. Displacement parameters (Å^2) for vanadio-oxy-chromium-dravite

	U^{11}	U^{22}	U^{33}	U^{23}	U^{13}	U^{12}	U_{eq}/U_{iso}[a]
Site			**Sample PR76**				
X	0.0215(4)	0.0215(4)	0.0200(5)	0	0	0.0107(2)	0.0210(3)
Y	0.00567(8)	0.00550(7)	0.00806(7)	–0.00037(3)	–0.00075(5)	0.00283(4)	0.00639(5)
Z	0.00432(8)	0.00477(8)	0.00596(7)	0.00044(5)	0.00004(5)	0.00218(6)	0.00506(5)
B	0.0063(3)	0.0076(5)	0.0087(4)	0.0013(3)	0.00065(17)	0.0038(2)	0.00739(19)
T	0.00488(9)	0.00441(9)	0.00684(8)	–0.00051(6)	–0.00037(7)	0.00229(7)	0.00539(5)
O1	0.0072(3)	0.0072(3)	0.0084(5)	0	0	0.00361(17)	0.0076(2)
O2	0.0065(2)	0.0047(3)	0.0094(3)	0.0011(2)	0.00054(12)	0.00233(16)	0.00707(14)
O3	0.0114(4)	0.0114(3)	0.0072(3)	0.00050(13)	0.0010(3)	0.00570(19)	0.01002(15)
O4	0.0075(2)	0.0153(4)	0.0097(3)	–0.0010(3)	–0.00051(14)	0.0076(2)	0.00995(15)
O5	0.0146(4)	0.0068(2)	0.0093(3)	0.00060(14)	0.0012(3)	0.0073(2)	0.00936(15)
O6	0.0091(2)	0.0072(2)	0.0063(2)	–0.00079(17)	–0.00057(17)	0.0042(2)	0.00752(10)
O7	0.0070(2)	0.0059(2)	0.0100(2)	–0.00154(17)	–0.00212(18)	0.00074(19)	0.00872(10)
O8	0.0046(2)	0.0088(3)	0.0172(2)	0.00360(19)	0.00141(19)	0.0028(2)	0.01042(11)
H3							0.015[a]
			Sample 1973				
X	0.0248(4)	0.0248(4)	0.0193(7)	0	0	0.0124(2)	0.0229(4)
Y	0.00595(7)	0.00574(5)	0.00687(10)	–0.00027(3)	–0.00053(6)	0.00297(4)	0.00616(4)
Z	0.00489(7)	0.00518(7)	0.00501(9)	0.00039(5)	0.00006(5)	0.00243(5)	0.00506(5)
B	0.0069(3)	0.0076(4)	0.0070(6)	0.0013(4)	0.00065(18)	0.0038(2)	0.0071(2)
T	0.00559(8)	0.00528(8)	0.00577(12)	–0.00057(7)	–0.00039(7)	0.00267(6)	0.00556(5)
O1	0.0070(3)	0.0070(3)	0.0076(8)	0	0	0.00348(16)	0.0072(2)
O2	0.0067(2)	0.0053(3)	0.0072(5)	0.0012(3)	0.00059(13)	0.00267(14)	0.00655(15)
O3	0.0113(3)	0.0107(2)	0.0053(4)	0.00027(14)	0.0005(3)	0.00563(17)	0.00904(15)
O4	0.0082(2)	0.0160(4)	0.0080(4)	–0.0005(3)	–0.00027(16)	0.00799(19)	0.00983(15)
O5	0.0157(4)	0.0074(2)	0.0078(5)	0.00057(16)	0.0011(3)	0.00787(18)	0.00940(16)
O6	0.0094(2)	0.0070(2)	0.0055(3)	–0.00045(19)	–0.00002(19)	0.00380(18)	0.00743(11)
O7	0.0073(2)	0.0067(2)	0.0087(3)	–0.00170(19)	–0.0016(2)	0.00100(17)	0.00866(11)
O8	0.0055(2)	0.0096(2)	0.0141(3)	0.0039(2)	0.0013(2)	0.00339(19)	0.00987(12)
H3							0.014[a]

[a] Equivalent (U_{eq}) and isotropic (U_{iso}) displacement parameters; H-atom was constrained to have a U_{iso} 1.5 times the U_{eq} value of the O3 oxygen.

X-ray powder diffraction

The X-ray powder-diffraction pattern for a small quantity of the vanadio-oxy-chromium-dravite sample (PR76) was collected using a Panalytical X'pert powder diffractometer equipped with an X'celerator silicon-strip detector. The range 5–70° (2θ) was scanned with a step-size of 0.017° during 4 h using a sample spinner with the sample mounted on a background-free holder. The diffraction data (in angstroms for Cu*K*α, $\lambda\alpha_1$ = 1.54060 Å), corrected using Si as an internal standard, are listed in Table 5. Since very limited amounts of sample material were available, only the stronger lines could be recorded.

Electron microprobe analysis

Electron microprobe analyses of the crystals used for X-ray diffraction refinements were obtained by wavelength-dispersive spectroscopy with a Cameca SX50 instrument at the "Istituto di Geologia Ambientale e Geoingegneria CNR" (Rome, Italy), operating at an accelerating potential of 15 kV and a sample current of 15 nA, with a 10 μm beam diameter. Minerals and synthetic compounds were used as standards: wollastonite (Si, Ca), magnetite (Fe), rutile (Ti), corundum (Al), vanadinite (V), fluorphlogopite (F), periclase (Mg), jadeite (Na), K-feldspar (K), sphalerite (Zn), metallic Cr, Mn, and Cu. The overlap corrections and the PAP routine were applied. The results, which are summarized in Table 6, represent mean values of 10 spot analyses. In accordance with the documented very low concentration of Li in dravitic samples (e.g., Henry et al. 2011), the Li_2O content was assumed to be insignificant. Mn and Cu and were found to be below their respective detection limits (0.03 wt%) in both studied samples.

Infrared spectroscopy

A homogeneous vanadio-oxy-chromium-dravite crystal (sample PR76) was measured by Fourier transform infrared (FTIR) absorption spectroscopy in the wavenumber range 2000–5000 cm^{-1} using a Bruker Equinox 55 spectrometer equipped with a NIR source, a CaF_2 beam-splitter and an InSb detector. Polarized spectra with a resolution of 4 cm^{-1} were obtained parallel and perpendicular to the **c** axis using a wire-grid polarizer (KRS-5) and a circular measurement area of 100 μm diameter on a 34 μm thick doubly polished crystal plate that had been oriented parallel the **c** axis by morphology and optical microscopy. Fundamental (OH) absorption bands polarized parallel to the **c** axis direction of tourmalines may be exceptionally intense, and as often observed, it was not possible to thin the sample sufficiently to avoid off-scale absorption intensity for the strongest bands (Fig. 1). An upolarized spectrum was therefore obtained on a powdered crystal, which confirmed that the main band does not consist of multiple components.

Optical absorption spectroscopy

Polarized, room-temperature optical absorption spectra were recorded in the spectral range 270–1100 nm (37037–9091 cm^{-1}) on a 25 μm thick, doubly sided

TABLE 4. Selected bond distances (Å) for vanadio-oxy-chromium-dravite

Sample	PR76	PR1973
X-O2^{B,F} (×3)	2.5834(12)	2.5749(14)
X-O5^{B,F} (×3)	2.7389(10)	2.7398(10)
X-O4^{B,F} (×3)	2.8187(10)	2.8243(11)
<X-O>	2.714	2.713
Y-O1	1.9583(7)	1.9565(8)
Y-O6^{C} (×2)	1.9960(6)	1.9871(7)
Y-O2^{B} (×2)	2.0302(5)	2.0240(6)
Y-O3	2.0919(9)	2.0803(9)
<Y-O>	2.017	2.010
Z-O8^{E}	1.9542(6)	1.9650(6)
Z-O7^{E}	1.9746(6)	1.9808(7)
Z-O8	1.9779(6)	1.9786(7)
Z-O6	1.9966(6)	2.0078(7)
Z-O7^{D}	2.0116(6)	2.0120(6)
Z-O3	2.0480(4)	2.0524(5)
<Z-O>	1.994	1.999
B-O8^{A} (×2)	1.3617(9)	1.3603(9)
B-O2	1.3969(16)	1.3972(15)
<B-O>	1.373	1.373
T-O7	1.5992(6)	1.5998(6)
T*-O6	1.6151(6)	1.6144(8)
T-O4	1.6292(3)	1.6283(4)
T-O5	1.6428(4)	1.6438(4)
<T-O>	1.622	1.622
H3-O3	0.855(18)	0.86(2)

Notes: Standard uncertainty in parentheses. Superscript letters: A = (y – x, y, z); B = (y – x, –x, z); C = (x, x – y, z); D = (y – x + 1/3, –x + 2/3, z + 2/3); E = (–y + 2/3, x – y + 1/3, z + 1/3); F = (–y, x – y, z). Transformations relate coordinates to those of Table 2.
* Positioned in adjacent unit cell.

TABLE 5. X-ray powder diffraction data for vanadio-oxy-chromium-dravite (sample PR76)

I_{meas} (%)	d_{meas} (Å)	d_{cal} (Å)	*hkl*
100	6.509	6.519	101
19	5.060	5.067	021
19	4.629	4.650	300
31	4.293	4.289	211
40	4.022	4.027	220
53	3.564	3.564	012
47	3.022	3.021	122
42	2.611	2.610	051
19	2.225	2.225	502
42	2.171	2.173	033
40	2.075	2.072	152
27	1.948	1.947	342
16	1.688	1.689	063
16	1.538	1.538	054

Notes: I_{meas} = measured intensity, d_{meas} = measured interplanar spacing; d_{calc} = calculated interplanar spacing; *hkl* = reflection indices. Estimated errors in d_{meas}-spacing range from 0.02 Å for large *d*-values to 0.003 Å for small *d*-values.

polished (100) platelet of a tourmaline single crystal (sample PR76) at a spectral resolution of 1 nm using an AVASPEC-ULS2048X16 spectrometer attached via a 400 μm UV optical fiber to a Zeiss Axiotron UV-microscope. A 75 W Xenon arc lamp served as illuminating source and Zeiss Ultrafluar 10× lenses served as objective and condenser. A UV-quality Glan-Thompson prism with a working range from 250 to 2700 nm (40 000 to 3704 cm^{-1}) was used as polarizer. The size of the circular measure aperture was 64 μm in diameter. The wavelength scale of the spectrometer was calibrated against Ho_2O_3-doped and Pr_2O_3/Nd_2O_3-doped standards (Hellma glass filters 666F1 and 666F7) with an accuracy better than 15 cm^{-1} in the wavelength range 300–1100 nm. Recorded spectra were fitted using the Jandel PeakFit 4.12 software assuming Gaussian peak shapes.

RESULTS AND DISCUSSION

General comment

The present crystal-structure refinements and electron microprobe analyses were obtained from the same individual crystals from the two samples (PR76 and PR1973). However, complementary powder X-ray diffraction data, FTIR spectra, optical absorption spectra, and refractive indices for sample PR76 were recorded from coexisting crystals. Small differences in composition are likely to occur between these crystals.

TABLE 6. Chemical composition of vanadio-oxy-chromium-dravite

Sample	PR76	PR1973
SiO_2 wt%	32.75(20)	32.27(12)
TiO_2	bdl	0.07(1)
B_2O_3	9.56[a]	9.40[a]
Al_2O_3	7.64(21)	4.54(19)
Cr_2O_3	12.87(37)	24.32(41)
V_2O_3	24.36(35)	14.88(27)
Fe_2O_3	0.42(10)[b]	0.86(5)[b]
MgO	7.19(24)	7.75(11)
ZnO	bdl	0.10(5)
CaO	bdl	0.05(1)
Na_2O	2.52(6)	2.71(3)
K_2O	0.24(3)	0.08(1)
F	0.25(10)	0.49(14)
H_2O	2.40[a]	2.33[a]
–O≡F	–0.11	–0.21
Total	100.10	99.63
Atomic proportions normalized to 31 anions		
Si apfu	5.95(4)	5.97(3)
Ti^{4+}	–	0.010(2)
B	3.00	3.00
Al	1.64(4)	0.99(4)
Cr^{3+}	1.85(5)	3.56(5)
V^{3+}	3.55(5)	2.21(4)
Fe^{3+}	0.06(2)	0.12(1)
Mg	1.95(6)	2.14(3)
Zn	–	0.014(7)
Ca	–	0.010(3)
Na	0.89(2)	0.97(1)
K	0.06(1)	0.018(2)
F	0.14(6)	0.29(8)
OH	2.91	2.87

Notes: Errors for oxides are standard deviations (in parentheses) of 10 spot analyses. Standard errors for the atomic proportions (in parenteheses) were calculated by error-propagation theory; bdl = below detection limits; apfu = atoms per formula unit.
[a] Calculated by stoichiometry.
[b] Calculated as Fe^{3+} (see text).

Determination of atomic proportions

In agreement with the structural refinement results, the boron content was assumed to be stoichiometric in both vanadio-oxy-chromium-dravite samples (B = 3.00 apfu). In fact, both the site-scattering results and the bond lengths of *B* and *T* are consistent with the *B* site fully occupied by boron and no amount of B at the *T* site. All iron was calculated as Fe^{3+} because this seems to be the dominant valence of iron in Cr-rich tourmaline (Bosi et al. 2013b). Note that due to the relatively low concentrations of Fe, uncertainty on its oxidation state has small influence on the overall charge calculations. The (OH) content can then be calculated by charge balance with the assumption $(T + Y + Z) = 15.00$. The atomic proportions were calculated on this assumption (Table 6). The excellent match between the number of electrons per formula unit (epfu) derived from chemical and structural analysis supports this procedure, respectively: 281.4 and 280.6 epfu for sample PR76; 288.0 and 287.7 epfu for sample PR1973.

Site populations

The anion site populations in the studied samples follow the general preference suggested for tourmaline (e.g., Grice and Ercit 1993; Henry et al. 2011): the O3 site (V position in the general

formula) is occupied by (OH) and O^{2-}, while the O1 site (W position in the general formula) is occupied by O^{2-} and F. The cation distribution at the *T*, *Y*, and *Z* sites was optimized by using a least-squares program to minimize the residuals between calculated and observed data (based on the chemical and structural analysis). Site-scattering values, octahedral, and tetrahedral mean bond-distances [i.e., <*Y*-O>, <*Z*-O>, and <*T*-O>] were calculated as the linear contribution of each cation multiplied by its ideal bond-distance (Table 7). More details about the ideal distances as well as about the optimization procedure may be found in Bosi et al. (2004) and Bosi and Lucchesi (2004, 2007). The robustness of this approach was confirmed by another optimization procedure (Wright et al. 2000), which led to very similar cation distributions (Table 7). This result represents another example of convergence of these two procedures to similar solutions for tourmaline (e.g., Bosi and Lucchesi 2007; Filip et al. 2012; Bosi et al. 2012a, 2013a).

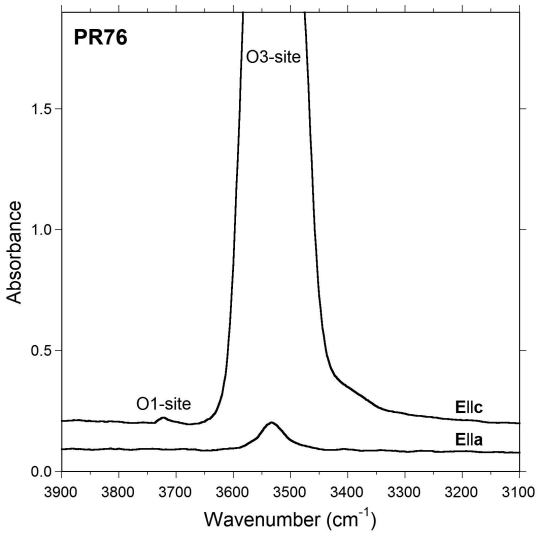

FIGURE 1. Polarized FTIR absorption spectra in the (OH)-stretching region of vanadio-oxy-chromium-dravite (sample PR76), vertically offset for clarity. Sample thickness 34 μm. The main band around 3535 cm^{-1} is truncated for the **c** direction due to excessive absorption intensity. Spectral ranges were bands related to (OH) in the O1- and O3-sites are expected are indicated.

The empirical structural formulas are as follows:

sample PR76,
$^{X}(Na_{0.89}K_{0.06}\square_{0.05})\ ^{Y}(V^{3+}_{2.77}Mg_{0.17}Fe^{3+}_{0.06})$
$^{Z}(Cr^{3+}_{1.85}Al_{1.59}V^{3+}_{0.78}Mg_{1.78})\ ^{T}[(Si_{5.95}Al_{0.05})O_{18}]$
$^{B}(BO_3)_3\ ^{V}(OH_{2.91}O_{0.09})\ ^{W}(O_{0.86}F_{0.14})$;

sample PR1973,
$^{X}(Na_{0.97}K_{0.02}Ca_{0.02})\ ^{Y}(V^{3+}_{2.21}Cr^{3+}_{0.54}Fe^{3+}_{0.12}Mg_{0.11}Ti^{4+}_{0.01}Zn_{0.01})$
$^{Z}(Cr^{3+}_{3.01}Al_{0.96}Mg_{2.03})\ ^{T}[(Si_{5.99}Al_{0.03})O_{18}]$
$^{B}(BO_3)_3\ ^{V}(OH_{2.87}O_{0.13})\ ^{W}(O_{0.71}F_{0.29})$.

The bond-valence analysis is consistent with the optimized structural formulas. Bond-valence calculations, using the formula and bond-valence parameters from Brown and Altermatt (1985), are reported in Table 8.

Crystal chemistry

The chemical composition of samples PR76 and PR1973 is consistent with tourmalines belonging to the alkali group, oxy-subgroup 3 (Henry et al. 2011). They are Na-dominant at the *X* site, oxygen-dominant at the W position, V^{3+} is the dominant cation at *Y*; Cr^{3+} is the dominant cation at *Z* and Mg is the dominant divalent cation at *Z*. The end-member formula may therefore be represented as $NaV_3(Cr_4Mg_2)Si_6O_{18}(BO_3)_3(OH)_3O$. Because no tourmalines have yet been documented as V^{3+}- and Cr^{3+}-dominant at *Y* and *Z*, respectively, this tourmaline can be classified as a new species. Its closest end-member composition of a valid tourmaline species is that of oxy-chromium-dravite (Bosi et al. 2012a), ideally $NaCr_3(Cr_4Mg_2)Si_6O_{18}(BO_3)_3(OH)_3O$. The name vanadio-oxy-chromium-dravite may hence be assigned for the chemical composition, following Henry et al. (2011). The prefix *vandio* represents the substitution, at the *Y* site, relative to the root composition of oxy-chromium-dravite.

Although there exists a small degree of V^{3+}, Cr^{3+}, and Mg

TABLE 7. Cation site populations (apfu), mean atomic numbers, and mean bond lengths (Å) for vanadio-oxy-chromium-dravite

Site	Site population	Mean atomic number		Mean bond length	
		refined	calculated	refined	calculated[a]
	Sample PR76				
X	0.89 Na + 0.06 K + 0.05□	11.02(7)	10.81		
Y	2.77 V^{3+} + 0.17 Mg + 0.06 Fe^{3+}	22.40(4)	22.42	2.017	2.023
	(2.74 V^{3+} + 0.24 Mg + 0.02 Fe^{3+})[b]				
Z	1.85 Cr^{3+} + 1.59 Al + 1.78 Mg + 0.78 V^{3+}	17.24(4)	17.40	1.994	1.990
	(1.82 Cr^{3+} + 1.65 Al + 1.74 Mg + 0.78 V^{3+})[b]				
T	5.95 Si + 0.05 Al	14[c]	13.99	1.622	1.621
B	3 B	5[c]	5		
	Sample PR1973				
X	0.97 Na + 0.02 K + 0.01□	10.93(7)	11.22		
Y	2.21 V^{3+} + 0.54 Cr^{3+} + 0.12 Fe^{3+} + 0.11 Mg + 0.01 Zn + 0.01 Ti^{4+}	23[c]	22.97	2.010	2.014
	(2.20 V^{3+} + 0.57 Cr^{3+} + 0.12 Fe^{3+} + 0.10 Mg + 0.02 Zn)[b]				
Z	3.01 Cr^{3+} + 2.03 Mg + 0.96 Al	18.12(4)	18.19	1.999	1.997
	(2.98 Cr^{3+} + 2.04 Mg + 0.98 Al + 0.03 Ti^{4+})[b]				
T	5.97 Si + 0.03 Al	14[c]	13.99	1.622	1.621
B	3 B	5[c]	5		

Notes: apfu = atoms per formula unit.
[a] Calculated using the ionic radii of Bosi and Lucchesi (2007).
[b] Site populations optimized by the procedure of Wright et al. (2000).
[c] Fixed in the final stages of refinement.

TABLE 8. Bond valence calculations (valence unit) for vanadio-oxy-chromium-dravite

Site	X	Y	Z	T	B	Σ
			PR76			
O1		$0.55^{\times3}\rightarrow$				1.65
O2	$0.13^{\times3}\downarrow$	$0.46^{\times2}\downarrow\rightarrow$			0.93	1.97
O3		0.39	$0.39^{\times2}\rightarrow$			1.17
O4	$0.07^{\times3}\downarrow$			$0.99^{\times2}\rightarrow$		2.04
O5	$0.08^{\times3}\downarrow$			$0.95^{\times2}\rightarrow$		1.99
O6		$0.50^{\times2}\downarrow$	0.45	1.02		1.97
O7			0.47			
			0.43	1.07		1.97
O8			0.47			
			0.50		$1.03^{\times2}\downarrow$	2.00
Σ	0.84	2.85	2.71	4.03	2.99	
MFV	0.94	2.92	2.70	3.99	3.00	
			PR1973			
O1		$0.53^{\times3}\rightarrow$				1.60
O2	$0.13^{\times3}\downarrow$	$0.46^{\times2}\downarrow\rightarrow$			0.93	1.98
O3		0.40	$0.39^{\times2}\rightarrow$			1.18
O4	$0.06^{\times3}\downarrow$			$0.99^{\times2}\rightarrow$		2.04
O5	$0.08^{\times3}\downarrow$			$0.95^{\times2}\rightarrow$		1.98
O6		$0.51^{\times2}\downarrow$	0.44	1.03		1.97
O7			0.47			
			0.43	1.07		1.97
O8			0.47			
			0.49		$1.03^{\times2}\downarrow$	1.99
Σ	0.82	2.88	2.69	4.03	2.99	
MFV	1.01	2.96	2.66	3.99	3.00	

Note: MFV = mean formal valence from site populations.

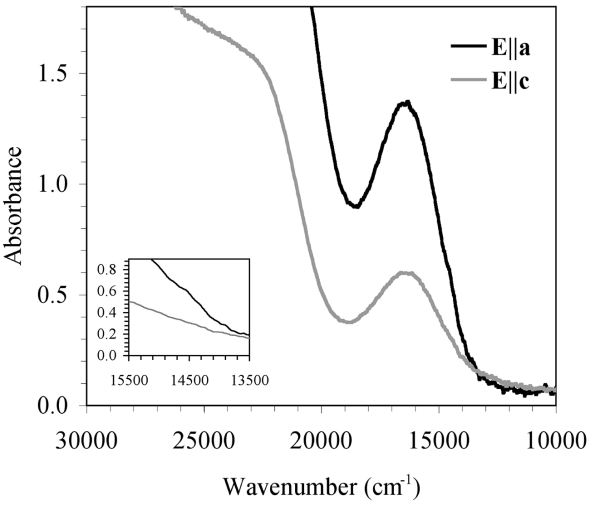

FIGURE 2. Polarized electronic spectra for vanadio-oxy-chromium-dravite (sample PR76). Sample thickness: 25 µm. The inset in the lower left corner shows in detail the spectral range where sharp spin-forbidden Cr^{3+}-bands are characteristic features in spectra of Cr-dominant tourmaline.

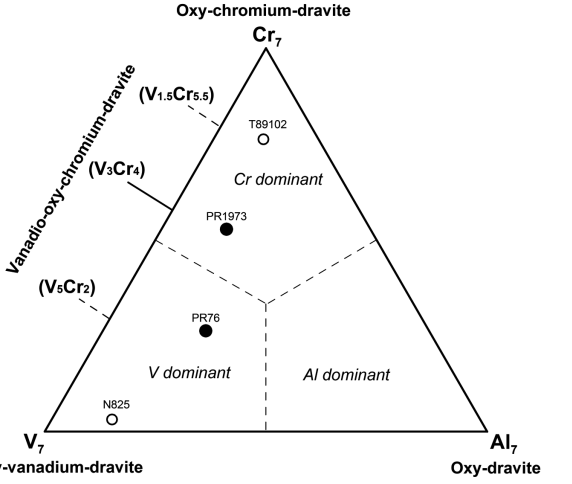

FIGURE 3. Ternary diagram in terms of Al-V-Cr at (*Y* + *Z*) sites for oxy-tourmalines. Black circles: present samples. White circles: sample T89102, oxy-chromium-dravite (Bosi et al. 2012a); and sample N825, oxy-vanadium-dravite (Bosi et al. 2013a). Note that (Al +V + Cr) at the (*Y*+Z) sites can add up only to 7 apfu, the remaining two apfu being Mg.

disorder over *Y* and *Z*, the structural formulas of samples PR76 and PR1973 indicate a clear preference of V^{3+} for the *Y* site, while Cr^{3+} and Mg prefer the *Z* site. Aluminum is completely ordered at the Z site. The O1 site population, characterized by O^{2-} with minor concentration of F, shows the absence of (OH) contents. This finding is consistent with the observation of extremely weak absorption bands occurring at wavenumbers higher than 3650 cm^{-1} in the infrared spectrum (Fig. 1), typically ascribed to the O1 site (see below).

Infrared spectroscopy

Spectra recorded in polarized mode perpendicular and parallel to the crystallographic **c** axis show an intense band around 3535 cm^{-1} and a very weak band at 3725 cm^{-1}, both polarized in the **c** direction (Fig. 1). The main band around 3535 cm^{-1} can be related to the local arrangement ($^{Y}V^{3+}\,{}^{Z}R\,{}^{Z}R$)-O3, i.e., to the occurrence of (OH) at the V position of the tourmaline general formula (O3-site in the structure). Note that no significant absorption bands occur at frequencies greater than 3650 cm^{-1}. This is consistent with the absence (or insignificant concentrations) of (OH) at the W position (O1-site in the structure) (cf. Gonzalez-Carreño et al. 1988; Bosi et al. 2012b, 2013b).

Optical absorption spectroscopy

The polarized electronic spectra show two intense and broad absorption bands observed at ~440 and 610 nm superimposed on an intense UV absorption (Fig. 2). Ligand field theory predicts that energies of absorption bands caused by spin-allowed electronic *d-d* transitions of octahedrally coordinated V^{3+} and Cr^{3+} should be comparable. The positions of the two intense bands in the present spectra are indeed close to those of bands caused by spin-allowed electronic *d-d* transitions in octahedrally coordinated Cr^{3+} in tourmaline (Taran et al. 1993; Ertl et al. 2008; Bosi et al. 2013b), but there exists several diagnostic differences. The recorded bands occur at distinctly higher wavelengths than the spin-allowed absorption bands caused by Cr^{3+} at the *Z*-site (425 and 574 nm; Taran et al. 1993) or the *Y*-site (430 and 590 nm; Bosi et al. 2013b) in tourmaline and, in addition to this, the diagnostic, narrow, spin-forbidden Cr^{3+}-bands at ~680 nm (Taran et al. 1993; Bosi et al. 2013b) are barely discernible in the present spectra (Fig. 2). Comparable diagnostic differences were noted in the spectra of a set of V- and Cr-rich (OH)-bearing tourmaline samples (olenite and uvite) with variable V/Cr-ratios by Ertl et al. (2008). Consequently, the broad and intense absorption bands at ~440 and 610 nm observed in the present spectra of vanadio-oxy-

TABLE 9. Comparative data for oxy-chromium-dravite, vanadio-oxy-chromium-dravite, and oxy-vanadium-dravite

	Oxy-chromium-dravite	Vanadio-oxy-chromium-dravite	Oxy-vanadium-dravite
a (Å)	16.05–16.11	16.13	16.19
c	7.32–7.37	7.38	7.41
V (Å³)	1634–1656	1662	1683
Space group	*R*3*m*	*R*3*m*	*R*3*m*
Optic sign	Uniaxial (–)	Uniaxial (–)	Uniaxial (–)
ω	1.765	1.767	1.786
ε	1.715	1.710	1.729
Streak	Green	Emerald-green	Yellowish-brownish
Color	Emerald-green	Green	Dark green to black
Pleochroism	O = dark-green E = yellow-green	O = dark green E = pale green	O = dark brownish green E = yellowish green
Reference	Bosi et al. (2012a)	This work	Reznitsky et al. (2001); Bosi et al. (2013a)

Notes: The range in unit-cell parameters for oxy-chromium-dravite represents data for two different samples (Bosi et al. 2012a).

chromium-dravite are mainly caused by spin-allowed *d-d* transitions in octahedrally coordinated V^{3+}. Contributions from absorption at slightly lower wavelengths caused by octahedrally coordinated Cr^{3+} mainly result in broadening of these V^{3+}-related absorption bands.

Compositional boundaries of vanadio-oxy-chromium-dravite

The plot of the *Z*- and *Y*-site cations in the ternary diagram for the Al-Cr-V^{3+} subsystem show, of course, that vanadio-oxy-chromium-dravite is ^{Z}Cr-dominant and ^{Y}V-dominant. More interesting, however, is the triangular plot in terms of Al-Cr-V^{3+} at *Y* and *Z*, showing that vanadio-oxy-chromium-dravite can be either Cr^{3+}-dominant (sample PR1973) or V^{3+}-dominant (sample PR76) (Fig. 3). This latter plot type displays the occurrence of three end-members along the full solid solution between the Cr^{3+} and V^{3+} apices: oxy-chromium-dravite, vanadio-oxy-chromium-dravite, and oxy-vanadium-dravite, for which comparative data are reported in Table 9. These end-members are related by the substitution $V^{3+} \leftrightarrow Cr^{3+}$ at the Y position (vanadio-oxy-chromium-dravite ↔ oxy-chromium-dravite) and $V^{3+} \leftrightarrow Cr^{3+}$ at the Z position (oxy-vanadium-dravite ↔ vanadio-oxy-chromium-dravite), while their compositional boundaries are at: (1) $^{Y+Z}(V_5Cr_2)$, corresponding to $Na^{Y}(V_3)^{Z}(V_2Cr_2Mg_2)Si_6O_{18}(BO_3)_3(OH)_3O$; (2) $^{Y+Z}(V_{1.5}Cr_{5.5})$, corresponding to $Na^{Y}(V_{1.5}Cr_{1.5})^{Z}(Cr_4Mg_2)Si_6O_{18}(BO_3)_3(OH)_3O$. Consequently, and assuming that V^{3+} and Cr^{3+} are completely ordered, oxy-chromium-dravite is characterized by V^{3+} contents less than 1.5 apfu, vanadio-oxy-chromium-dravite is characterized by V^{3+} contents between 5 and 1.5 apfu, and oxy-vanadium-dravite is characterized by V^{3+} contents larger than 5 apfu.

With regard to the relations among Al, Cr^{3+}, and V^{3+} in oxy-tourmalines, the current chemical data support complete solid-solution involving V^{3+}, Cr^{3+}, and Al (Reznitsky et al. 2001; Bosi et al. 2004, 2013a, 2013b).

ACKNOWLEDGMENTS

Chemical analyses were carried out with the kind assistance of M. Serracino to whom the authors express their gratitude. L. Reznitskii was supported by a grant from Russian Foundation for Basic Research (project 13-05-00258). We thank F. Colombo and G.R. Rossman for their useful suggestions that improved the manuscript.

REFERENCES CITED

Agrosì, G., Bosi, F., Lucchesi, S., Melchiorre, G., and Scandale, E. (2006) Mn-tourmaline crystals from island of Elba (Italy): Growth history and growth marks. American Mineralogist, 91, 944–952.

Bačík, P., Uher, P., Ertl, A., Jonsson, E., Nysten, P., Kanický, V., and Vaculovič, T. (2012) Zoned REE enriched dravite from a granitic pegmatite in Forshammar Bergslagen Province, Sweden an EPMA, XRD and LA-ICP-MS study. Canadian Mineralogist, 50, 825–841.

Bosi, F. (2008) Disordering of Fe^{2+} over octahedrally coordinated sites of tourmaline. American Mineralogist, 93, 1647–1653.

——— (2010) Octahedrally coordinated vacancies in tourmaline: a theoretical approach. Mineralogical Magazine, 74, 1037–1044.

——— (2011) Stereochemical constraints in tourmaline: from a short-range to a long-range structure. Canadian Mineralogist, 49, 17–27.

——— (2013) Bond-valence constraints around the O1 site of tourmaline. Mineralogical Magazine, 77, 343–351.

Bosi, F., and Lucchesi, S. (2004) Crystal chemistry of the schorl-dravite series. European Journal of Mineralogy, 16, 335–344.

——— (2007) Crystal chemical relationships in the tourmaline group: structural constraints on chemical variability. American Mineralogist, 92, 1054–1063.

Bosi, F. and Skogby, H. (2013) Oxy-dravite, $Na(Al_2Mg)(Al_5Mg)(Si_6O_{18})(BO_3)_3(OH)_3O$, a new mineral species of the tourmaline supergroup. American Mineralogist, 98, 1442–1448.

Bosi, F., Lucchesi, S., and Reznitskii, L. (2004) Crystal chemistry of the dravite-chromdravite series. European Journal of Mineralogy, 16, 345–352.

Bosi, F., Balić-Žunić, T., and Surour, A.A. (2010) Crystal structure analysis of four tourmalines from the Cleopatra's Mines (Egypt) and Jabal Zalm (Saudi Arabia), and the role of Al in the tourmaline group. American Mineralogist, 95, 510–518.

Bosi, F., Reznitskii, L., and Skogby, H. (2012a) Oxy-chromium-dravite, $NaCr_3(Cr_4Mg_2)(Si_6O_{18})(BO_3)_3(OH)_3O$, a new mineral species of the tourmaline supergroup. American Mineralogist, 97, 2024–2030.

Bosi, F., Skogby, H., Agrosì, G., and Scandale, E. (2012b) Tsilaisite, $NaMn_3Al_6(Si_6O_{18})(BO_3)_3(OH)_3OH$, a new mineral species of the tourmaline supergroup from Grotta d'Oggi, San Pietro in Campo, island of Elba, Italy. American Mineralogist, 97, 989–994.

Bosi, F., Reznitskii, L., and Sklyarov, E.V. (2013a) Oxy-vanadium-dravite, $NaV_3(V_4Mg_2)(Si_6O_{18})(BO_3)_3(OH)_3O$: crystal structure and redefinition of the "vanadium-dravite" tourmaline. American Mineralogist, 98, 501–505.

Bosi, F., Skogby, H., Hålenius, U., and Reznitskii, L. (2013b) Crystallographic and spectroscopic characterization of Fe-bearing chromo-alumino-povondraite and its relations with oxy-chromium-dravite and oxy-dravite. American Mineralogist, 98, 1557–1564.

Brown, I.D., and Altermatt, D. (1985) Bond-valence parameters obtained from a systematic analysis of the Inorganic Crystal Structure Database. Acta Crystallographica, B41, 244–247.

Ertl, A., Rossman, G.R., Hughes, J.M., Ma, C., and Brandstätter, F. (2008) V^{3+}-bearing, Mg-rich, strongly disordered olenite from a graphite deposit near Amstall, Lower Austria: A structural, chemical and spectroscopic investigation. Neues Jahrbuch für Mineralogie Abhandlungen, 184, 243–253.

Filip, J., Bosi, F., Novák, M., Skogby, H., Tuček, J., Čuda, J., and Wildner, M. (2012) Redox processes of iron in the tourmaline structure: example of the high-temperature treatment of Fe^{3+}-rich schorl. Geochimica et Cosmochimica Acta, 86, 239–256.

Foit, F.F. Jr. (1989) Crystal chemistry of alkali-deficient schorl and tourmaline structural relationships. American Mineralogist, 74, 422–431.

Gonzalez-Carreño, T., Fernandez, M., and Sanz, J. (1988) Infrared and electron microprobe analysis in tourmalines. Physics and Chemistry of Minerals, 15, 452–460.

Grice, J.D., and Ercit, T.S. (1993) Ordering of Fe and Mg in the tourmaline crystal structure: the correct formula. Neues Jahrbuch für Mineralogie, Abhandlungen, 165, 245–266.

Hawthorne, F.C. (1996) Structural mechanisms for light-element variations in tourmaline. Canadian Mineralogist, 34, 123–132.

——— (2002) Bond-valence constraints on the chemical composition of tourmaline. Canadian Mineralogist, 40, 789–797.

Hawthorne, F.C., and Henry, D. (1999) Classification of the minerals of the tourmaline group. European Journal of Mineralogy, 11, 201–215.

Henry, D.J., and Dutrow, B.L. (2011) The incorporation of fluorine in tourmaline: Internal crystallographic controls or external environmental influences? Canadian Mineralogist, 49, 41–56.

Henry, D.J., Novák, M., Hawthorne, F.C., Ertl, A., Dutrow, B., Uher, P., and Pezzotta, F. (2011) Nomenclature of the tourmaline supergroup minerals. American Mineralogist, 96, 895–913.

Lussier, A.J., Aguiar, P.M., Michaelis, V.K., Kroeker, S., Herwig, S., Abdu, Y., and Hawthorne, F.C. (2008) Mushroom elbaite from the Kat Chay mine, Momeik, near Mogok, Myanmar: I. Crystal chemistry by SREF, EMPA, MAS NMR and Mössbauer spectroscopy. Mineralogical Magazine, 72, 747–761.

Lussier, A.J., Hawthorne, F.C., Aguiar, P.M., Michaelis, V.K., and Kroeker, S. (2011a) Elbaite-liddicoatite from Black Rapids glacier, Alaska. Periodico di Mineralogia, 80, 57–73.

Lussier, A.J., Abdu, Y. Hawthorne, F.C., Michaelis, V.K., Aguiar, P.M., and Kroeker, S. (2011b) Oscillatory zoned liddicoatite from Anjanabonoina, central Mada-

gascar. I. Crystal chemistry and structure by SREF and ^{11}B and ^{27}Al MAS NMR spectroscopy. Canadian Mineralogist, 49, 63–88.
Novák, M., Povondra, P., and Selway, J.B. (2004) Schorl-oxy-schorl to dravite-oxy-dravite tourmaline from granitic pegmatites; examples from the Moldanubicum, Czech Republic. European Journal of Mineralogy, 16, 323–333.
Novák, M., Škoda, P., Filip, J., Macek, I., and Vaculovič, T. (2011) Compositional trends in tourmaline from intragranitic NYF pegmatites of the Tøebíč Pluton, Czech Republic; electron microprobe, Mössbauer and LA-ICP-MS study. Canadian Mineralogist, 49, 359–380.
Reznitsky, L.Z., Sklyarov, E.V., Ushchapovskaya, Z.V., Nartova, N.V., Kashaev, A.A., Karmanov, N.S., Kanakin, S.V., Smolin, A.S., and Nekrosova, E.A. (2001) Vanadiumdravite, $NaMg_3V_6[Si_6O_{18}][BO_3]_3(OH)_4$, a new mineral of the tourmaline group. Zapiski Vsesoyuznogo Mineralogicheskogo Obshchestva, 130, 59–72 (in Russian).
Sheldrick, G.M. (2008) A short history of SHELX. Acta Crystallographica, A64, 112–122.
Skogby, H., Bosi, F., and Lazor, P. (2012) Short-range order in tourmaline: a vibrational spectroscopic approach to elbaite. Physics and Chemistry of Minerals, 39, 811–816.
Taran, M.N., Lebedev, A.S., and Platonov, A.N. (1993) Optical absorption spectroscopy of synthetic tourmalines. Physics and Chemistry of Minerals, 20, 209–220.
van Hinsberg, V.J., and Schumacher, J.C. (2011) Tourmaline as a petrogenetic indicator mineral in the Haut-Allier metamorphic suite, Massif Central, France. Canadian Mineralogist, 49, 177–194.
van Hinsberg, V.J., Henry, D.J., and Marschall, H.R. (2011) Tourmaline: an ideal indicator of its host environment. Canadian Mineralogist, 49, 1–16.
Wright, S.E., Foley, J.A., and Hughes, J.M. (2000) Optimization of site occupancies in minerals using quadratic programming. American Mineralogist, 85, 524–531.

Manuscript received April 23, 2013
Manuscript accepted September 11, 2013
Manuscript handled by Fernando Colombo